

# Rational Design of Dual Peptides Targeting Ghrelin and Y<sub>2</sub> Receptors to Regulate Food Intake and Body Weight

Tom-Marten Kilian,<sup>†</sup> Nora Klötting,<sup>‡</sup> Ralf Bergmann,<sup>§</sup> Sylvia Els-Heindl,<sup>†</sup> Stefanie Babilon,<sup>†</sup> Mathieu Clément-Ziza,<sup>||</sup> Yixin Zhang,<sup>⊥</sup> Annette G. Beck-Sickinger,<sup>†</sup> and Constance Chollet<sup>\*,†,⊥,#</sup>

<sup>†</sup>Faculty of Biosciences, Pharmacy and Psychology, Institute of Biochemistry, Universität Leipzig, Brüderstrasse 34, 04103 Leipzig, Germany

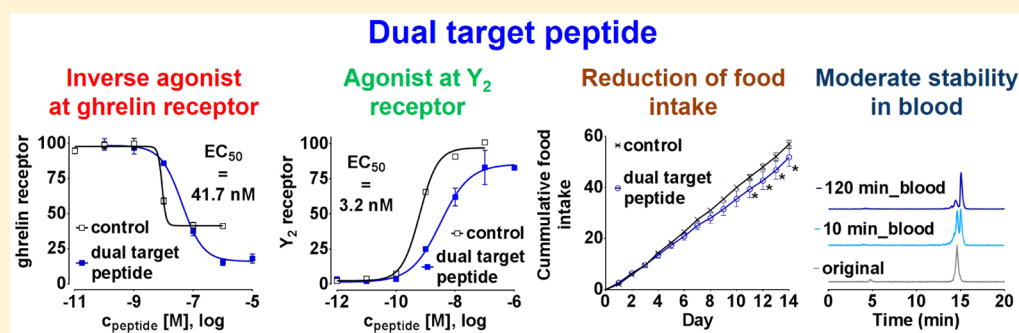
<sup>‡</sup>Integrated Research and Treatment Center Adiposity Diseases (IFB), Core Unit "Animal Models", Universität Leipzig, Liebigstrasse 21, 04103 Leipzig, Germany

<sup>§</sup>Department of Radiopharmaceutical and Chemical Biology, Institute of Radiopharmaceutical Cancer Research, Helmholtz-Zentrum Dresden-Rossendorf, P.O. Box 510119, 01314 Dresden, Germany

<sup>||</sup>CECAD - Cluster of Excellence, University of Cologne, Joseph-Stelzmann-Str. 26, 50931 Cologne, Germany

<sup>⊥</sup>B CUBE-Center for Molecular Bioengineering, Technische Universität Dresden, Arnoldstrasse 18, 01307 Dresden, Germany

## Supporting Information



**ABSTRACT:** Ghrelin and Y<sub>2</sub> receptors play a central role in appetite regulation inducing opposite effects. The Y<sub>2</sub> receptor induces satiety, while the ghrelin receptor promotes hunger and weight gain. However, the food regulating system is tightly controlled by interconnected pathways where redundancies can lead to poor efficacy and drug tolerance when addressing a single molecule. We developed a multitarget strategy to synthesize dual peptides simultaneously inhibiting the ghrelin receptor and stimulating the Y<sub>2</sub> receptor. Dual peptides showed dual activity *in vitro*, and one compound induced a slight diminution of food intake in a rodent model of obesity. In addition, stability studies in rats revealed different behaviors between the dual peptide and its corresponding monomers. The Y<sub>2</sub> receptor agonist was unstable in blood, while the dual peptide showed an intermediate stability compared to that of the highly stable ghrelin receptor inverse agonist.

## ■ INTRODUCTION

The regulation of food intake involves permanent communication between the gastrointestinal tract (gut) and the central nervous system (CNS) in a complex and integrated network.<sup>1</sup> Hence, gut peptides are key messengers between the different parts of the gastrointestinal tract and in the gut–brain axis. Principally, peptide hormones are released from the gut and pancreas to mediate the short- and long-term regulation of hunger and satiety, food intake, energy homeostasis, and body weight. They communicate energy and feeding statutes to central checkpoints involved in food regulation and energy homeostasis, mainly the POMC/AgRP neurons in the arcuate nucleus of the hypothalamus and some neuronal populations of the brainstem. Although not fully understood, the signaling between the gut and the CNS is thought to occur through areas with a leaky blood–brain barrier, i.e., the median eminence

near the arcuate nucleus and the area postrema in the brainstem, as well as via the vagus nerve.<sup>2</sup>

Obesity leads to a sustained dysregulation of energy homeostasis and disruption of gut peptide expression.<sup>3</sup> Expression levels of satiety hormones such as PYY, GLP-1, and PP as well as the orexigenic peptide ghrelin decrease in obesity. Various studies also reported that food intake and body weight can be reduced in obese humans or rodents by the administration of satiety hormones.<sup>4</sup> On the contrary, ghrelin stimulates appetite when administrated to both lean and obese subjects, and a low-calorie diet or weight loss raise ghrelin levels and up-regulate ghrelin receptor expression.<sup>5,6</sup> In addition, a sustained modification of gut peptide profiles is observed after

**Received:** November 3, 2014

**Published:** April 23, 2015

intestinal bypass operations with elevated postprandial concentrations of the satiety hormones GLP-1 and PYY and a 75% decrease in ghrelin levels.<sup>7,8</sup>

In this context, gastrointestinal peptides have emerged as promising targets to treat obesity.<sup>9,10</sup> However, redundancies in the food regulating system can lead to poor efficacy and drug tolerance.<sup>11</sup> Moreover, antiobesity drugs should always be considered as a chronic treatment excluding side effects in a long-term perspective. Therefore, using drug combination for obesity is currently considered as a strategy of choice, although only few have been investigated using gastrointestinal peptides.<sup>12,13</sup>

In this article, we present a rational multitarget approach to simultaneously block the food regulating system at different levels (Figure 1). The rationale of multitargeting is indeed to

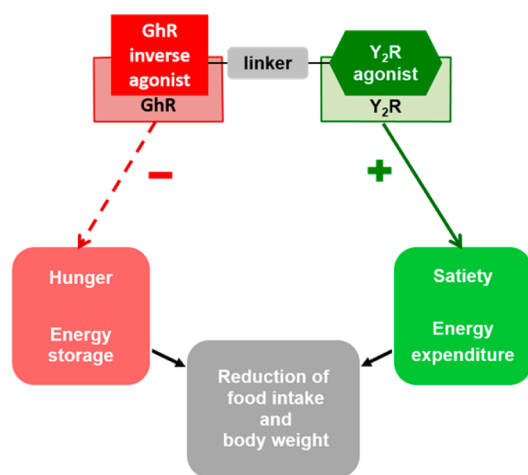


**Figure 1.** Dual targeting strategy of the ghrelin and  $Y_2$  receptors.

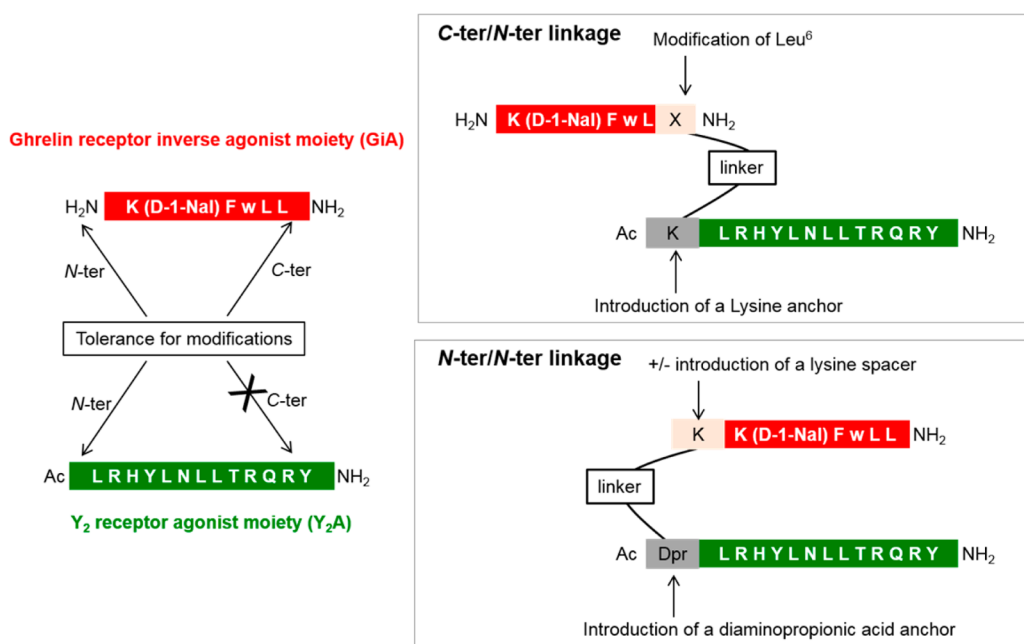
mimic polytherapy, while bypassing issues related to drug combination.<sup>14</sup> Hence, dual peptides simultaneously inhibiting the ghrelin receptor and activating the  $Y_2$  receptor were

designed and evaluated *in vitro* and *in vivo*. Both receptors are indeed considered as promising drug targets for obesity.<sup>15–17</sup> PYY(3–36) is the endogenous ligand of the  $Y_2$  receptor and acts as a direct satiety signal with a short-term effect on appetite regulation. Ghrelin is a unique orexigenic signal from the periphery that mediates hunger, promotes weight gain, and stimulates energy storage. Thus,  $Y_2$  receptor agonists and, more recently, potent ghrelin receptor antagonists and inverse agonists have been developed.<sup>18</sup> The simultaneous targeting of ghrelin and  $Y_2$  receptors is based on the colocalizations of both receptors on the same neuronal population, the NPY/AgRP neurons, in the arcuate nucleus of hypothalamus.

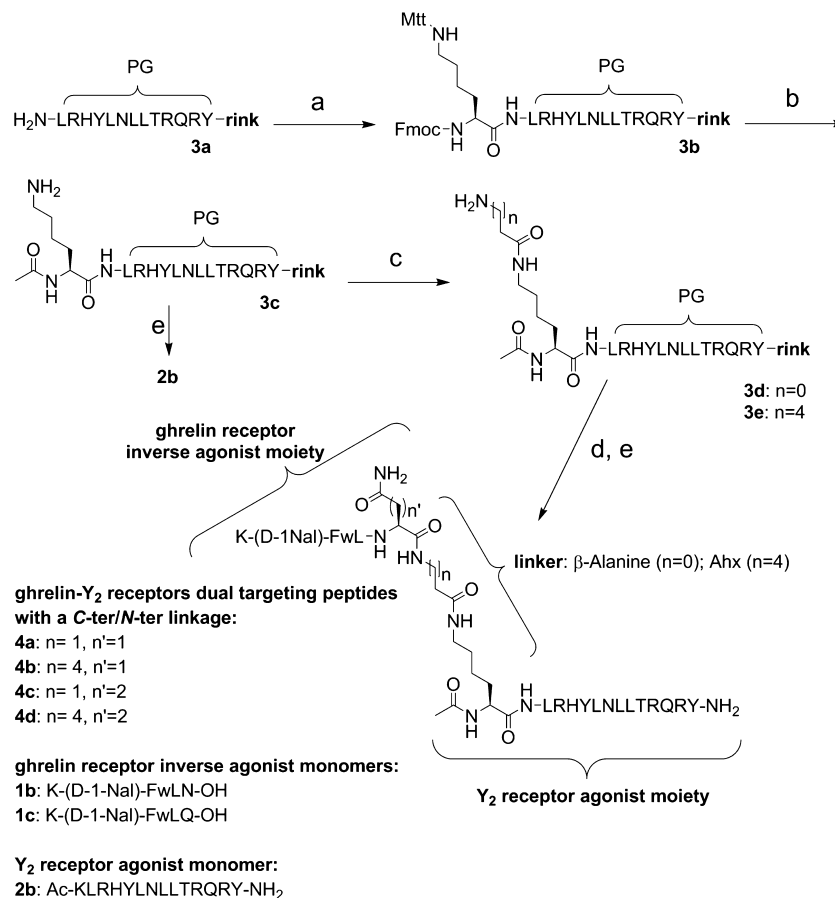
## ■ RATIONAL DESIGN OF GHRELIN- $Y_2$ RECEPTOR DUAL TARGETING PEPTIDES

**Selection of a Ghrelin Inverse Agonist.** The hexapeptide K-(D-1-Nal)-FwLL-NH<sub>2</sub> **1a** was selected as the ghrelin receptor targeting moiety as it possesses a very high inverse agonist potency and high affinity toward the ghrelin receptor. It also significantly reduced food intake in rats in acute food intake studies.<sup>19</sup> Previous structure–activity relationship (SAR) studies showed that the peptide core was sensitive to modifications.<sup>19,20</sup> Lys<sup>1</sup> and the aromatic core -(D-1-Nal)-Fw are essential for receptor recognition and potency and cannot be modified. The amidated C-terminus also needs to be preserved. However, the N-terminus and the C-terminal leucine allow modifications and could tolerate anchoring a linker (Figure 2).

**Selection of a  $Y_2$  Receptor Agonist.** PYY(3–36) is the endogenous ligand selective to the  $Y_2$  receptor. Importantly, truncation of the N-terminal sequence (3–21) only resulted in a 4- to 5-fold decrease in potency toward the receptor.<sup>21</sup> However, maintaining an exclusive selectivity toward  $Y_2$  over other receptors of the Y family is challenging but essential as  $Y_1$  and  $Y_5$  receptors induce orexigenic signals and thus achieve opposite effects from  $Y_2$ .<sup>22</sup> Hence, Ac-[L<sup>31</sup>]-PYY(24–36) **2a** was selected from the literature as it presents good selectivity



**Figure 2.** Design of ghrelin- $Y_2$  receptor dual targeting peptides.

Scheme 1. Synthesis of Ghrelin- $Y_2$  Receptor Dual Targeting Peptides 4a–d with a C-ter/N-ter Linkage<sup>a</sup>

<sup>a</sup>Reagents and conditions: (a) Fmoc-L-Lys(Mtt)-OH, Oxyma, DIC, DMF, r.t., 2 h; (b) (i) piperidine, 20% in DMF,  $2 \times 15$  min; (ii) Ac<sub>2</sub>O, DIPEA, DCM, r.t., 30 min; (iii) TFA/TIPS/DCM, 1/5/94, r.t.,  $15 \times 2$  min; (c) (i) Fmoc-L- $\beta$ -Ala-OH or Fmoc-Ahx-OH, Oxyma, DIC, DMF, r.t., 2 h; (ii) piperidine, 20% in DMF,  $2 \times 15$  min; (d) manual/automated peptide elongation; (e) TFA/thioanisole/thiocresol, 90/5/5, r.t. 3 h.

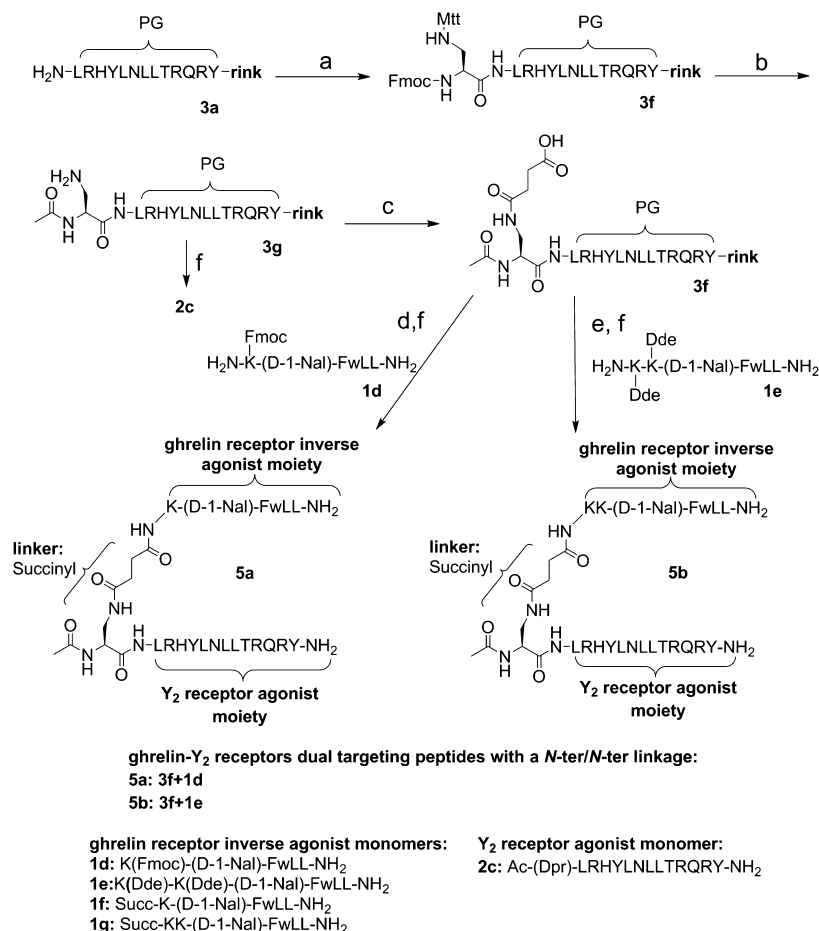
and potency toward the  $Y_2$  receptor ( $IC_{50} = 3.9 \pm 0.4$  nM in human neuroblastoma SMS-KAN cells that only express the  $Y_2$  receptor).<sup>23</sup> Moreover, PEGylated derivatives of 2a significantly decreased food intake and body weight after administration to rodents.<sup>24,25</sup> According to the numerous SAR studies on the PYY motif, the C-terminal section of the peptide is essential for activity and selectivity.<sup>26</sup> However, the N-terminal region of truncated PYY analogues tolerates modification and thus the introduction of a linker.

## RESULTS

**Synthesis of Ghrelin- $Y_2$  Receptor Dual Targeting Peptides with a C-ter/N-ter Linkage.** [ $L^{31}$ ]-PYY(24–36) 3a was elongated on Rink amide resin. Addition of a Mtt-protected lysine at its N-terminus affords 3b. N-Terminal acetylation followed by selective Mtt deprotection at N<sup>6</sup> of Lys<sup>23</sup> led to 3c, and 3d–e were finally obtained by coupling an amino hexanoic acid or a  $\beta$ -alanine linker (Scheme 1). In order to connect the ghrelin receptor inverse agonist moiety via its C-terminus, the sequence of the hexapeptide K-(D-1-Nal)-FwLL-NH<sub>2</sub> 1a was modified. Leu<sup>6</sup> was replaced with an asparagine or a glutamine so that the carboxamide side chain could mimic the amidated C-terminus of the native monomer 1a. Dual peptides 4a–d were obtained accordingly, by elongating 3d–e with K-(D-1-Nal)-FwLN- or K-(D-1-Nal)-FwLQ- on solid support and then cleaving from the resin. The modified monomers K-(D-1-

Nal)-FwLN-OH 1b, K-(D-1-Nal)-FwLQ-OH 1c, and Ac-[K<sup>23</sup>,L<sup>31</sup>]-PYY(23–36) 2b were also synthesized on solid support for biological assays.

**Synthesis of Ghrelin- $Y_2$  Receptor Dual Targeting Peptides with a N-ter/N-ter Linkage.** [ $L^{31}$ ]-PYY(24–36) 2a was elongated on Rink amide resin. Addition of Mtt-protected diamino propionic acid (Dpr) at its N-terminus afforded 3f (Scheme 2). N-Terminal acetylation followed by selective Mtt deprotection at N<sup>7</sup> of Dpr<sup>23</sup> led to 3g and allowed the insertion of a succinyl linker to obtain 3h. In order to connect the ghrelin receptor inverse agonist moieties via its N-terminus, two monomers 1d and 1e were also synthesized on solid support and cleaved from the resin. An Fmoc protecting group for 1d and Dde protecting groups for 1e were maintained at lysines side chains to avoid side reactions with free amino groups. Hence, 1d and 1e were coupled to 3h at the free carboxylic group. To spare the starting peptides 1d and 1e, the peptide bond was formed with equimolar amount of 3h and 1d–e, and the reaction was repeated once. After Fmoc- or Dde-cleavage, final cleavage from the resin, and side chain deprotection, dual peptides 5a and 5b were obtained in solution. Because of the low excess of starting peptides 1d and 1e, conversion of 3h was never complete, and a mixture of 3h and 5a–b was obtained after cleavage from the solid support. Nevertheless, dual peptides 5a and 5b could be easily purified.

Scheme 2. Synthesis of Ghrelin- $Y_2$  Receptor Dual Targeting Peptides 5a–b with a N-ter/N-ter Linkage<sup>a</sup>

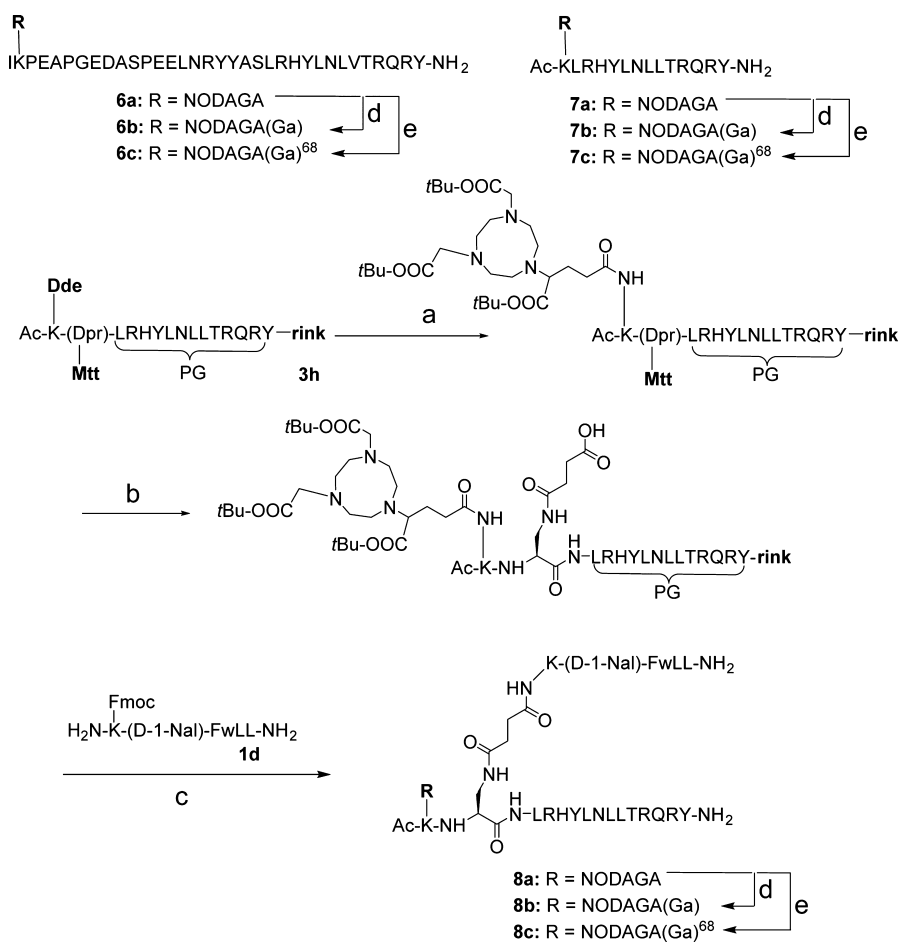
<sup>a</sup>Reagents and conditions: (a) Fmoc-L-Dpr(Mtt)-OH, Oxyma, DIC, DMF, r.t., 2 h; (b) (i) piperidine, 20% in DMF, 2 × 15 min; (ii) Ac<sub>2</sub>O, NEt<sub>3</sub>, DCM, r.t., 30 min; (iii) TFA/TIPS/DCM, 1/5/94, r.t., 15 × 2 min; (c) succinic anhydride, NEt<sub>3</sub>, DMF r.t., overnight; (d) (i) 1d, HOBt, DIC, DMF, r.t., overnight × 2; (ii) piperidine, 20% in DMF, 2 × 15 min; (e) (i) 1e, HOBt, DIC, DMF, r.t., overnight × 2; (ii) hydrazine 2% in DMF, 10 × 10 min; (f) TFA/thioanisole/thiocresol, 90/5/5, r.t. 3 h.

The monomers 1f, 1g, and Ac-[Dpr<sup>23</sup>;L<sup>31</sup>]-PYY(23–36) 2c were also synthesized on solid support for biological assays.

**Synthesis of Radiolabeled Peptides for Stability Assay.** In order to perform stability studies *in vivo*, PYY(3–36), 2a and 5a were functionalized with the bifunctional chelator NODAGA, according to a procedure previously optimized.<sup>27</sup> NODAGA-(BOC)<sub>3</sub> was directly bonded to a N<sup>ε</sup>-lysine of PYY(3–36) and 2a on solid support and led to the NODAGA-conjugates 6a and 7a after cleavage from the resin (Scheme 3). The NODAGA-conjugate 8a was obtained following the same synthesis path as 5a. Hence, the Y<sub>2</sub>R moiety 3h was elongated on a Rink amide resin. NODAGA(BOC)<sub>3</sub> was introduced at N<sup>ε</sup>-Lys<sup>1</sup> after selective Dde cleavage. A succinic linker was then coupled at N<sup>β</sup>-Dpr<sup>2</sup> after selective Mtt cleavage to allow for connecting ghrelin monomer 1d at the free carboxylic group. Complexation with cold Ga was performed by incubating the peptides with a solution of Ga(NO<sub>3</sub>)<sub>3</sub> in acetate buffer (pH 5) at 37 °C. The cold chelates 6–8b were directly purified by HPLC to remove the excess of metal and used for *in vitro* binding assays. For radiolabeling, conjugates 6–8a were incubated with <sup>68</sup>Ga(OAc)<sub>3</sub> in acetate buffer (pH 4.0 to 4.5) for 15 min at 37 °C and led to <sup>68</sup>Ga-radiotracers 6–8c in solution.

**In Vitro Potency at Ghrelin and Y<sub>2</sub> Receptors.** Potency of the dual peptides at the ghrelin receptor was evaluated with an inositol phosphate accumulation assay in COS-7 cells, stably expressing the human ghrelin receptor. A 44-fold to 55-fold drop in potency was observed for dual peptides 4a–b compared with that of control 1a (Table 1 and Figure 3A). Both compounds presented EC<sub>50</sub> in the submicromolar range (respectively, EC<sub>50</sub> = 331 nM and EC<sub>50</sub> = 267 nM). The corresponding monomer 1b also presented a 31-fold decreased potency compared with that of control 1a with an EC<sub>50</sub> = 189 nM. Compounds 4c–d were more potent but showed EC<sub>50</sub>, respectively, 17- and 15-fold higher than that of the control 1a (EC<sub>50</sub> = 100 nM and 88.3 nM, respectively). The corresponding monomer 1c presented potency in the same range with an EC<sub>50</sub> = 70.2 nM. Hence, replacement of Leu<sup>6</sup> of the ghrelin receptor inverse agonist 1a, and modification of the amidated C-terminus was moderately tolerated. Nevertheless, potency was less affected when (a) Leu<sup>6</sup> was replaced with Gln<sup>6</sup> than with Asn<sup>6</sup> (4c–d versus 4a–b) and (b) for monomers bearing a free carboxyl C-terminus than for the corresponding dual peptides (1b versus 4a–b and 1c versus 4c–d). Furthermore, in this series, derivatives with a hexanoyl linker showed slightly higher potencies than compounds with a β-alanine linker (4b versus 4a and 4d versus 4c).

**Scheme 3.** Synthesis of the NODAGA-Peptide Conjugates **6–8a**, the NODAGA(Ga)-Peptide Chelates **6–8b**, and the Corresponding NODAGA(Ga)<sup>68</sup>-Peptide Radiotracers **6–8c**<sup>a</sup>



<sup>a</sup>Reagents and conditions: (a) (i) hydrazine 2% in DMF, 10 × 10 min; (ii) NODAGA(BOC)<sub>3</sub>, HOBT, DIC, DMF; (b) (i) TFA/TIPS/DCM, 1/5/94, r.t., 15 × 2 min; (ii) succinic anhydride, NEt<sub>3</sub>, DMF r.t., overnight; (c) (i) **1d**, HOBT, DIC, DMF, r.t., overnight × 2; (ii) piperidine, 20% in DMF, 2 × 15 min; (iii) TFA/thioanisole/thiocresol, 90/5/5, r.t. 3 h; (d) Ga(NO<sub>3</sub>)<sub>3</sub>, pH 5.0, 37 °C, 30 min; (e) <sup>68</sup>Ga(OAc)<sub>3</sub>, pH 4.0–4.5, 37 °C, 15 min.

Higher potencies were obtained with dual peptides **5a–b** (Table 1 and Figure 3B). Compound **5a** showed an EC<sub>50</sub> = 41.7 nM, only 7-fold higher than that of control **1a**, and thus being the best dual peptide. However, **5b** was 20-fold less potent than **1a** (EC<sub>50</sub> = 109.6 nM) and thus equipotent to **4c–d**. The monomer **1f** and **1g** were more potent than the corresponding dual peptide but were, respectively, 5-fold and 10-fold less potent than control **1a** (EC<sub>50</sub> = 29.0 nM and 60.2 nM, respectively). Thus, introduction of an extra lysine at the *N*-terminus of the ghrelin inverse agonist sequence led to a drop in potency (**1g** and **5b**), whereas the direct connection of the succinic linker at the *N*-terminus maintained the potency in the low nanomolar range at the ghrelin receptor (**1f** and **5a**). Importantly, monomer **2b** targeting the Y<sub>2</sub> receptor was inactive at the ghrelin receptor.

Potency of the dual peptides at the Y<sub>2</sub> receptor was evaluated with an inositol phosphate accumulation assay in COS-7 cells stably coexpressing the human Y<sub>2</sub> receptor and a chimeric G<sub>i/q</sub> protein. Compounds **4a–b** were not tested at the Y<sub>2</sub> receptor due to their poor potency toward the ghrelin receptor. Dual peptides **4c–d** showed nanomolar potencies at the Y<sub>2</sub> receptor, with, respectively, EC<sub>50</sub> = 1.7 nM and EC<sub>50</sub> = 3.9 nM (Table 1 and Figure 4C). Potencies were nevertheless 3- and 6-fold

lower than that of control **2d**, and a slight decrease in efficacy was also observed (~85% versus 95%). The corresponding monomer **2b** was equipotent to control **2d** with EC<sub>50</sub> = 0.5 nM but presented a loss in efficacy (Eff = 68%). Potencies of dual peptides **5a–b** at the Y<sub>2</sub> receptor were in the nanomolar range, with, respectively, EC<sub>50</sub> = 3.2 nM and EC<sub>50</sub> = 2.0 nM, showing a 5- and 3-fold drop of potency compared with that of control **2d** (Table 1 and Figure 4D). The corresponding monomer **2c** was equipotent to control **2d** with EC<sub>50</sub> = 0.4 nM. In addition, **2c** and **5a–b** all showed decreased efficacies from 77% to 84% compared to that of control **2d**. Last, monomers **1c**, **1f**, and **1g** targeting the ghrelin receptor were inactive at the Y<sub>2</sub> receptor.

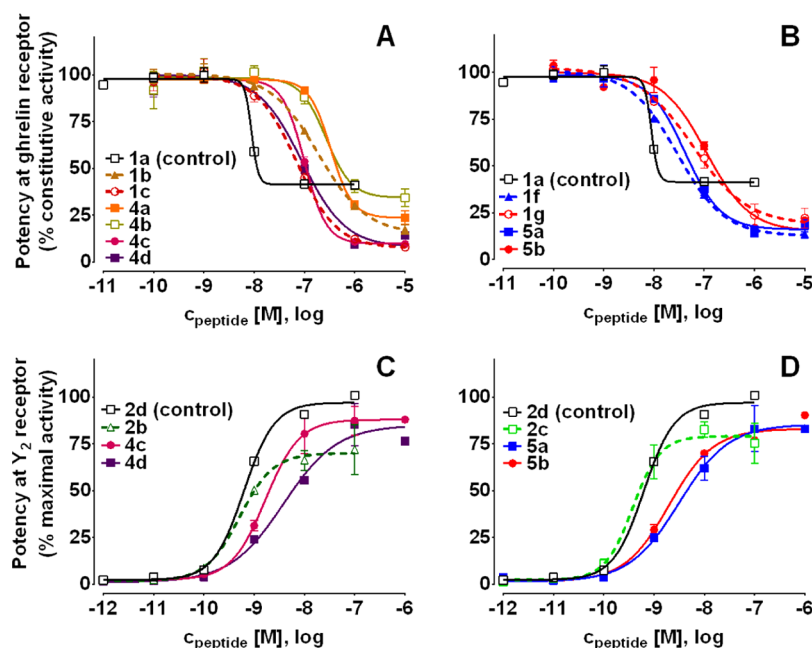
In conclusion, dual peptides with a *C*-ter/*N*-ter linkage presented low (**4a–b**) or moderate (**4c–d**) potency, in the submicromolar range, at the ghrelin receptor, while potency at the Y<sub>2</sub> receptor was maintained in the nanomolar range (**4c–d**). Dual peptides **5a–b** with *N*-ter/*N*-ter linkage showed distinct behavior. Compound **5a** expressed the highest potency at the ghrelin receptor, with only a 7-fold decrease compared with the control, while **5b** was moderately potent. Both compounds presented a high potency, in the nanomolar range at the Y<sub>2</sub> receptor.



Table 1. *In Vitro* Potency and Efficacy at the Ghrelin and Y<sub>2</sub> Receptors<sup>a</sup>

no.	structure	ghrelin receptor (GhR)				Y <sub>2</sub> receptor (Y <sub>2</sub> R)			
		EC <sub>50</sub> [nM]	pEC <sub>50</sub> ± SEM	x-fold over 1a	Eff [%]	n	EC <sub>50</sub> [nM]	pEC <sub>50</sub> ± SEM	x-fold over 2d
1a (control)	K-(D-1-Nal)-FwLL-NH <sub>2</sub>	6.0	8.2 ± 0.1	1	55 ± 3	4	n.d. <sup>b</sup>		
1b	K-(D-1-Nal)-FwLN-OH	189.2	6.7 ± 0.08	31	86 ± 4	2	n.d.		
1c	K-(D-1-Nal)-FwLQ-OH	70.2	7.2 ± 0.08	12	92 ± 5	2	>1000		
1f	Succ-K-(D-1-Nal)-FwLL-NH <sub>2</sub>	29.0	7.5 ± 0.07	5	88 ± 3	2	>1000		
1g	Succ-KK-(D-1-Nal)-FwLL-NH <sub>2</sub>	60.2	7.2 ± 0.1	10	84 ± 7	2	>1000		
2d (control)	SPEELNRYASLRHYLNLVTRQRYNH <sub>2</sub>	n.d.					0.6	9.2 ± 0.05	1.0
2b	Ac-KLRHYLNLTRQRY-NH <sub>2</sub>	>1000				2	0.5	9.3 ± 0.1	0.8
2c	Ac-(Dpr)-LRHYLNLTRQRY-NH <sub>2</sub>	n.d.					0.4	9.4 ± 0.1	0.6
4a	Ac-K[βala-NLwF-(D-1-Nal)-K]-LRHYLNLTRQRY-NH <sub>2</sub>	331.3	6.5 ± 0.05	55	74 ± 2	2	n.d.		
4b	Ac-K[Ahx-NLwF-(D-1-Nal)-K]-LRHYLNLTRQRY-NH <sub>2</sub>	266.8	6.6 ± 0.2	44	64 ± 7	2	n.d.		
4c	Ac-K[βala-QLwF-(D-1-Nal)-K]-LRHYLNLTRQRY-NH <sub>2</sub>	99.9	7.0 ± 0.02	17	88 ± 2	2	1.7	8.8 ± 0.1	3
4d	Ac-K[Ahx-QLwF-(D-1-Nal)-K]-LRHYLNLTRQRY-NH <sub>2</sub>	88.3	7.1 ± 0.1	15	85 ± 4	2	3.9	8.4 ± 0.2	6
5a	Ac-Dpr[Succ-K-(D-1-Nal)-FwLLNH <sub>2</sub> ]-LRHYLNLTRQRY-NH <sub>2</sub>	41.7	7.4 ± 0.08	7	82 ± 4	2	3.2	8.5 ± 0.2	5
5b	Ac-Dpr[Succ-KK-(D-1-Nal)-FwLLNH <sub>2</sub> ]-LRHYLNLTRQRY-NH <sub>2</sub>	109.6	7.0 ± 0.1	18	78 ± 5	2	2.0	8.7 ± 0.08	3

<sup>a</sup>EC<sub>50</sub> and pEC<sub>50</sub> ± SEM values were obtained from log(concentration)–response curves according to a 4 parameter logistic (4PL) nonlinear regression model and showed the potency of the peptides at the ghrelin receptor (GhR) and at the Y<sub>2</sub> receptor (Y<sub>2</sub>R). Efficacy values (Eff) are the mean ± SEM of Eff<sub>max</sub> – Eff<sub>min</sub>.<sup>b</sup> n.d.: not determined.



**Figure 3.** Concentration–response curves of 4a–d and 5a–b in the inositol phosphate turnover assay in COS-7 cells stably expressing the human ghrelin receptor (A,B) and in COS-7 cells stably coexpressing the human Y<sub>2</sub> receptor and a chimeric G<sub>i/q</sub> protein (C,D). The responses are expressed in % of constitutive activity of the ghrelin receptor or in % of maximum activity of the Y<sub>2</sub> receptor, and error-bars indicate SEM over two biological replicates.

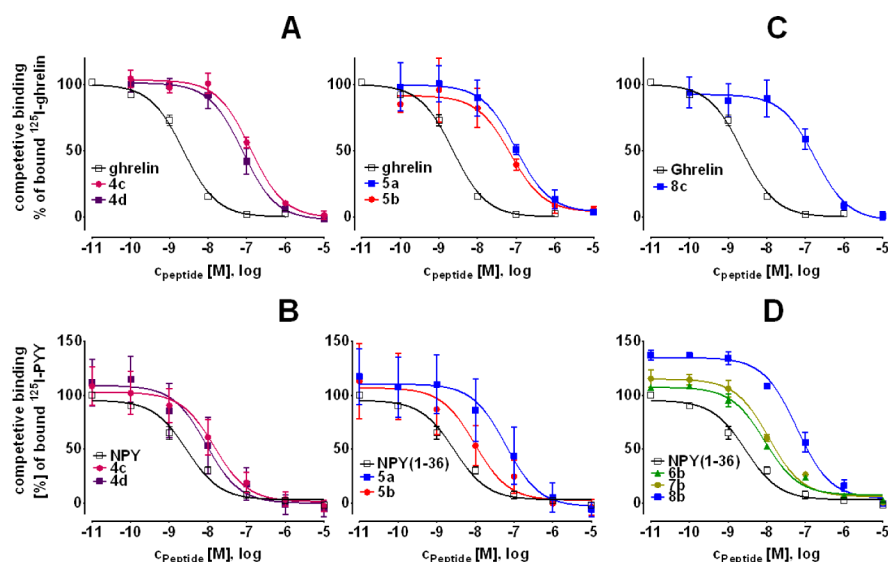


**Figure 4.** Concentration–response curves of 4c–d, 5a–b, and 6–8b in competitive binding assays performed with <sup>125</sup>I-ghrelin in COS-7 cells stably expressing the human ghrelin receptor (A,C) and with <sup>125</sup>I-PYY in HEK-293 cells stably expressing the human Y<sub>2</sub> receptor (B,D). The response is expressed in % of bound <sup>125</sup>I-ghrelin or % of bound <sup>125</sup>I-PYY, and error-bars indicate the SEM over at least two biological replicates.

#### **In Vitro Affinity at the Ghrelin and Y<sub>2</sub> Receptors.**

Competitive binding of the dual peptides 4c–d and 5a–b and the NODAGA(Ga)-chelates 6–8b was evaluated (i) at the ghrelin receptor with <sup>125</sup>I-ghrelin and (ii) at the Y<sub>2</sub> receptor with <sup>125</sup>I-PYY. All dual peptides showed a binding affinity in the submicromolar range (IC<sub>50</sub> = 70.4 to 126 nM) at the ghrelin receptor with a 31- to 55-fold shift compared with that of ghrelin (Figure 4A and Table 2). Hence, the decrease in binding affinities was comparable for the dual peptides with a C-ter/N-ter linkage (4c–d) and with a N-ter/N-ter linkage (5a–b). The binding affinity of all dual peptides was maintained in the nanomolar range at the Y<sub>2</sub> receptor, although

5a showed discrepancies (Figure 4B and Table 2). Compounds 4c–d and 5b presented only a 3- to 5-fold decrease in affinity compared with that of NPY (IC<sub>50</sub> = 9 to 14.7 nM), while a lower binding affinity toward the Y<sub>2</sub> receptor was observed for 5a (IC<sub>50</sub> = 61.4 nM).

Binding affinity of the NODAGA(Ga)-chelates 6–8b was also evaluated prior to stability studies *in vivo* (Figure 4C and D and Table 2). The Y<sub>2</sub> receptor agonists 6–7b derived from PYY(3–36) and 2a showed binding affinity only 3- to 4-fold lower than that of NPY for the Y<sub>2</sub> receptor (IC<sub>50</sub> = 8.8 and 11.3 nM, respectively). The dual targeting chelates 8b presented a binding affinity toward the Y<sub>2</sub> receptor similar to that of its

Table 2. *In Vitro* Affinity of the Dual Peptides 4c–d and 5a–b and of the NODAGA(Ga)-Chelates 6–8b toward Ghrelin and Y<sub>2</sub> receptors in Competitive Binding Assays<sup>a</sup>

no.	structure	ghrelin receptor (GhR)				Y <sub>2</sub> receptor (Y <sub>2</sub> R)			
		IC <sub>50</sub>	pIC <sub>50</sub> ± SEM	x-fold over ghrelin	n	IC <sub>50</sub>	pIC <sub>50</sub> ± SEM	x-fold over NPY	n
Ghrelin	control (GhR)	2.3	8.64 ± 0.06		3	n.d.			
NPY	control (Y <sub>2</sub> R)	n.d. <sup>b</sup>				2.8	8.55 ± 0.08		4
4c	Ac-K[ <sup>1</sup> ala-QwF-(D-1-Nal)-K]-LRHYLNLLTRQRY-NH <sub>2</sub>	126	6.90 ± 0.10	55	2	14.7	7.83 ± 0.25	5	3
4d	Ac-K[ <sup>1</sup> Abx-QwF-(D-1-Nal)-K]-LRHYLNLLTRQRY-NH <sub>2</sub>	78.2	7.11 ± 0.12	34	3	9	8.05 ± 0.32	3	3
5a	Ac-Dpr[Succ-K-(D-1-Nal)-FwLL-NH <sub>2</sub> ]-LRHYLNLLTRQRY-NH <sub>2</sub>	97.1	7.01 ± 0.20	42	2	61.4	7.2 ± 0.39	22	3
5b	Ac-Dpr[Succ-KK-(D-1-Nal)-FwLL-NH <sub>2</sub> ]-LRHYLNLLTRQRY-NH <sub>2</sub>	70.4	7.15 ± 0.25	31	2	9.7	8.02 ± 0.38	3	3
6b	[K <sup>4</sup> (NODAGA(Ga))]-PYY(3–36)	n.d.				8.8	8.05 ± 0.07	3	2
7b	Ac-K(NODAGA(Ga))-LRHYLNLLTRQRY-NH <sub>2</sub>	n.d.				11.3	7.95 ± 0.10	4	2
8b	Ac-K(NODAGA(Ga))-Dpr[Succ-K-(D-1-Nal)-FwLL-NH <sub>2</sub> ]-LRHYLNLLTRQRY-NH <sub>2</sub>	174	6.76 ± 0.20	76	3	60	7.22 ± 0.08	21	2

<sup>a</sup>EC<sub>50</sub> and pEC<sub>50</sub> ± SEM values were obtained from log(concentration)–response curves according to a 4PL nonlinear regression model and showed the binding affinity of the peptides at the ghrelin receptor (GhR) and at the Y<sub>2</sub> receptor (Y<sub>2</sub>R). <sup>b</sup>n.d.: not determined.

precursor 5a (IC<sub>50</sub> = 60 nM). In parallel, the binding affinity of 8b for the ghrelin receptor, although lower than that of 5a, remained in the same order of magnitude (IC<sub>50</sub> = 174 nM).

**Selectivity toward the Y<sub>2</sub> Receptor.** To determine the selectivity of the dual peptide 4c–d and 5a–b toward the Y<sub>2</sub> receptor over Y<sub>1</sub>, Y<sub>4</sub>, and Y<sub>5</sub> receptors, inositol phosphate accumulation was measured in COS-7 cells stably coexpressing the corresponding human Y receptor and a chimeric G<sub>i/q</sub> protein, for each compound, at 10<sup>−6</sup> M. All values were normalized over the NPY response at each receptor and expressed in % of NPY response at each receptor. These data showed the efficacy of the dual peptides at each receptor and could be compared with efficacy toward the Y<sub>2</sub> receptor (Figure 5). All dual peptides showed efficacies from 79 to 90% at the Y<sub>2</sub>

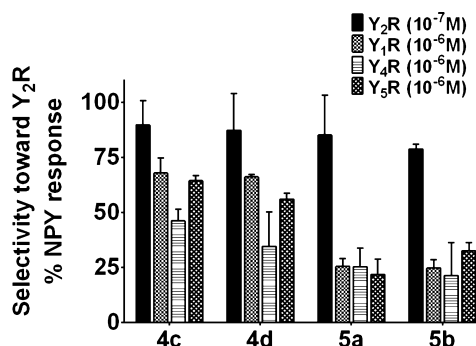
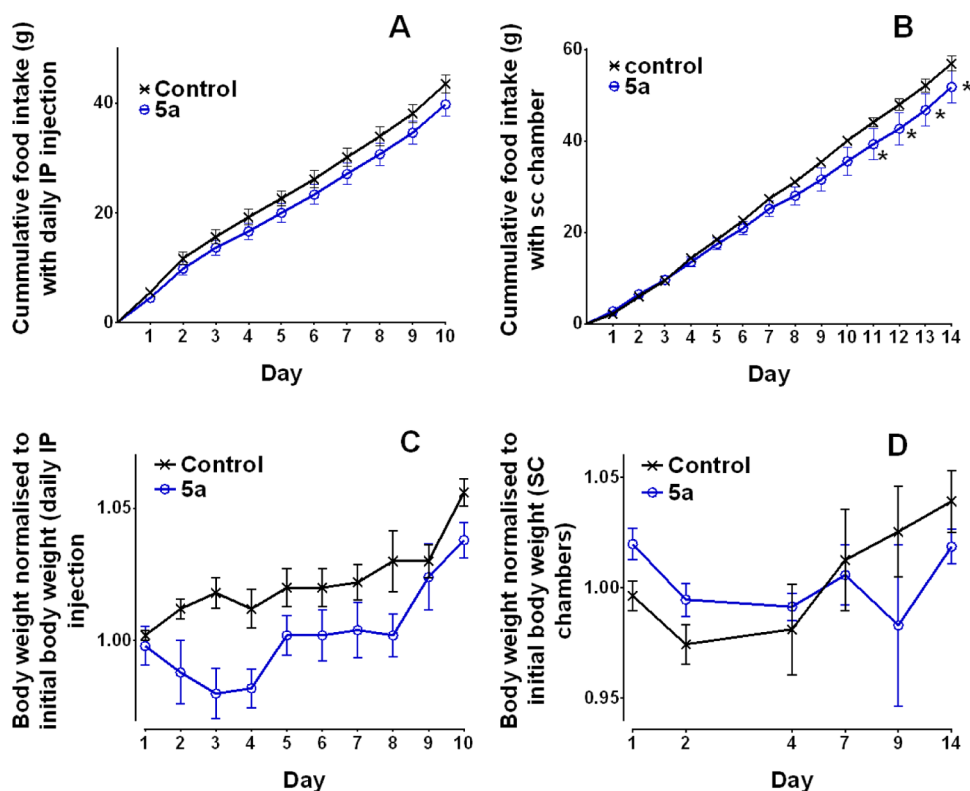


Figure 5. Selectivity of 4c–d and 5a–b toward the Y<sub>2</sub> receptor over Y<sub>1</sub>, Y<sub>2</sub>, Y<sub>4</sub>, and Y<sub>5</sub> receptors at high concentration. All compounds were tested in the inositol phosphate accumulation assay with COS-7 cells stably coexpressing the corresponding human Y receptor and a chimeric G<sub>i/q</sub> protein. The response is expressed in % of NPY response at each receptor, and error-bars indicate the SEM over two biological replicates.

receptor. Efficacies of dual peptides 4c and 4d were higher than 66% at the Y<sub>1</sub> receptor and higher than 56% at the Y<sub>5</sub> receptor. Efficacies at the Y<sub>4</sub> receptor were, respectively, 46% and 35%. Hence, the selectivity of 4c–d for the Y<sub>2</sub> receptor was relatively low. On the contrary, dual peptides 5a and 5b showed efficacies lower than 25% at the Y<sub>1</sub> and Y<sub>4</sub> receptors and up to 33% at Y<sub>5</sub> receptor. Thus, 5a and 5b showed a high selectivity toward the Y<sub>2</sub> receptor compared to that of the other Y receptors.

**Food Intake Assay.** According to the *in vitro* results, the dual peptide 5a presents the best dual potency and a moderate binding affinity at both ghrelin and Y<sub>2</sub> receptors. In addition, it possesses a good selectivity toward the Y<sub>2</sub> receptor over Y<sub>1</sub>, Y<sub>4</sub>, and Y<sub>5</sub> receptors. To further investigate its pharmacological interest, *in vivo* food intake assays were performed in diet-induced obese mice. Hence, freely fed mice were randomized in different groups and treated with (a) a saline solution (control group); (b) the ghrelin receptor inverse agonist 1a (K-(D-1-Nal)-FwLL-NH<sub>2</sub>); (c) hPYY(3–36); (d) the Y<sub>2</sub> receptor agonist 2a (Ac-LRHYLNLLTRQRY-NH<sub>2</sub>); (e) the dual targeting peptide 5a; and (f) coadministration of 1a + 2a. Cumulative food intake and body weight were measured for each group in parallel, and the significance of the effect was statistically assessed for each treatment. Acute subcutaneous (SC) administration of the drugs at 500 nM/kg or intraperitoneal (IP) injection at 50, 100, or 250 nM/kg did not significantly modify the feeding behavior nor the body weight of mice (data not shown). When the drugs were administrated by daily IP at 100 nM/kg for 10 days, repeated-measures





**Figure 6.** Cumulative food intake in obese C57BL/6 mice after (A) daily IP injection of 5a or saline solution (control) or (B) implantation of SC chambers in mice at D0 and slow release of 5a or saline solution (control). Body weight normalized to initial body weight of mice after (C) daily IP injection of 5a or saline solution (control) or (D) implantation of SC chambers in mice at D0 and slow release of 5a or saline solution (control). Error-bars indicate the SEM over five biological replicates. \* indicates a significant pairwise difference at 0.05 FDR.

ANOVA showed a significant drug treatment-by-time interaction for food intake and body weight (respectively,  $p < 0.0001$  and  $p = 0.013$ , Supporting Information, Tables S3 and S6). However, pairwise comparisons showed no persistent effects on food intake compared to that of the control (Figure 6A and Figure S1-A and Table S4, Supporting Information). Surprisingly, pairwise comparisons on the body weight normalized to initial body weight showed a significant increase of body weight for mice treated with PYY(3–36) compared to that of the control at days 7, 9, and 10 (Supporting Information, Table S7; respectively,  $p = 0.0306$ ,  $p = 0.0069$ , and  $p = 0.0427$ , multiple hypothesis adjusted  $p$ -value for the posthoc comparison of peptide PYY(3–36) versus the control). Nevertheless, no difference on bodyweight was observed for mice treated with 5a compared to that of the control group (Figure 6C and Supporting Information, Table S7). When mice were implanted with subcutaneous osmotic micropumps that slowly released the drugs at 0.25 nM/h for 14 days, data suggested a drug treatment-by-time effect on food intake and body weight (although not formally significant,  $p = 0.0732$  and  $p = 0.0663$ , respectively, Supporting Information, Tables S9 and S12). Pairwise comparisons to the control group further confirmed a small but significant decrease in food intake for the dual peptide 5a at the end of the treatment (Figure 6B and Supporting Information, Table S10;  $p = 0.049$ ,  $p = 0.0239$ ,  $p = 0.0225$ , and  $p = 0.0313$ , multiple hypothesis adjusted  $p$ -value for the posthoc comparison of peptide 5a to control at days 11 to 14). All other treatments did not show any significant differences in food intake compared to that of the control (see Supporting Information, Figures S1B and S1D for 1a, 2a, 1a + 2a and hPYY(3–36), and Supporting Information, Tables

S10 and S13). Hence, decrease of food intake was uniquely observed for the dual peptide 5a in chronic food intake studies.

**Metabolic Stability in Rats.** The metabolic stability of 6–8c was evaluated in rat arterial blood. Therefore, clearance of the total radioactivity was monitored after injection of the tracers (Figure 7A), and metabolite fractions were calculated for each tracer (Figure 7B) after quantification of the metabolites by HPLC analysis (Figure 7C). hPP(3–36) tracer 6c exhibited good stability in blood. Its metabolite fraction reached 22% within 30 min after injection and corresponded to a single metabolite that could be observed on the chromatogram. Tracer 6c also displayed relatively fast clearance in arterial blood with decreasing concentrations from 5.1 to 0.5% ID·mL<sup>-1</sup> within 30 min. Conversely, the Y<sub>2</sub> agonist tracer 7c presented a dramatically low metabolic stability in blood. The chromatogram showed a direct conversion of 7c into a major metabolite. Indeed, the metabolite fraction of 7c already represented 88% of the total 1 min after injection and metabolism was completed within 3 min. Accordingly, measurement of the blood clearance was not relevant for 7c as it did not reflect the concentration of the original compound. Last, tracer 8c, derived from the dual peptide 5a, was moderately stable in blood. Conversion of 8c into a major metabolite was visible on the chromatogram within 10 min after injection. The corresponding metabolite fraction represented 67% after 5 min and reached a plateau of 80% after 10 min. Nevertheless, blood clearance of 8c was slower than that for 6c and 7c. Hence, the concentration of 8c dropped from 5.4 to 1.1% ID·mL<sup>-1</sup> within 30 min.

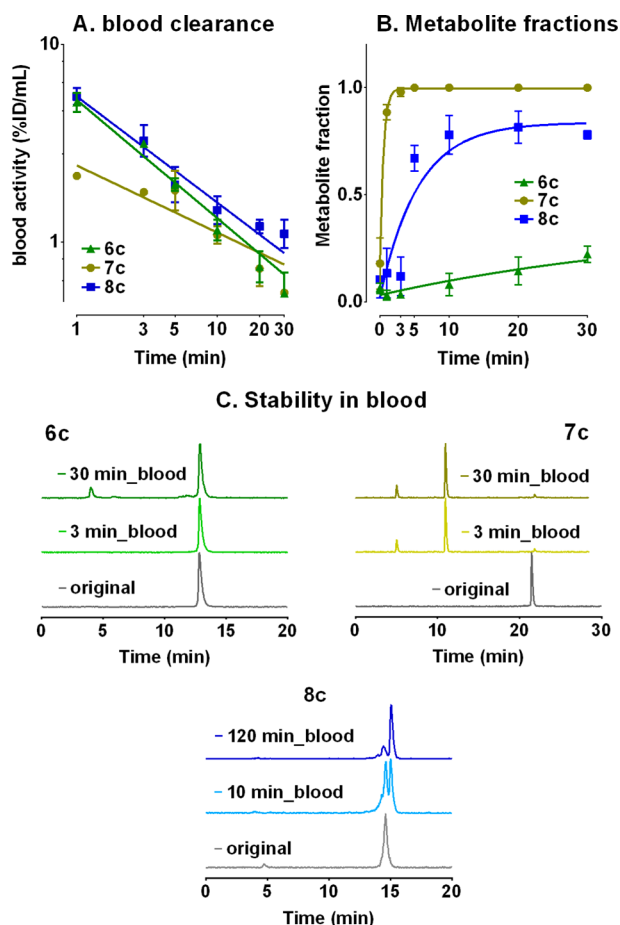


**Figure 7.** (A) Blood clearance, (B) radioactive metabolites, and (C) chromatograms of radiotracers 6–8c in blood after injection in rats. Error-bars indicate the SEM over two biological replicates. Curve for radioactive metabolites were fitted to a one-phase association kinetic.

## DISCUSSION

The aim of this study was to design dual peptides simultaneously targeting the  $Y_2$  and ghrelin receptors. Dual peptides were synthesized by connecting the ghrelin receptor inverse agonist **1a** to the  $Y_2$  receptor agonist **2a** via a linker. According to previous SAR studies on both ligands, C-ter/N-ter and N-ter/N-ter linkage was investigated. As speculated, the ghrelin inverse agonist sequence was sensitive to modifications. Although elongation of the ghrelin inverse agonist sequence seemed better tolerated at its N-terminus than its C-terminus, no general trends could be highlighted. Hence, the potency of all dual peptides followed the same trend as their corresponding monomers at the ghrelin receptor. Dual peptides **4a–d** with a C-ter/N-ter linkage exhibited various potencies. Compounds **4a–b** with Asn<sup>6</sup> instead of Leu<sup>6</sup> on the ghrelin inverse agonist moiety showed a drastic loss of potency, whereas the potency of **4c–d**, containing a Gln<sup>6</sup>, was maintained in the high nanomolar range. Dual peptides **5a–b**, possessing a N-ter/N-ter linkage, also exhibited different potencies while only differing by a lysine spacer at the N-terminus of the ghrelin inverse agonist moiety. Hence, **5a** presented the best potency at the ghrelin receptor (41.7 nM), whereas **5b** was only potent in the submicromolar range.

Interestingly, dual peptides **4c–d** (C-ter/N-ter linked) and **5a–b** (N-ter/N-ter linked) presented comparable binding affinities at the ghrelin receptor. This is in contradiction with

previous modeling studies showing that **1a** and short hexapeptide analogues adopted an L-shaped form and bound the receptor with their N-terminus pointing toward the binding pocket, while their C-terminus remained at the entrance of the pocket (C-out mode).<sup>19</sup> However, other modeling and docking experiments demonstrated that wFw-based analogues of **1a**, agonists or biased agonists at the ghrelin receptor, could bind in the main ligand-binding pocket in two opposite orientations. In the C-in mode, the C-terminal carboxamide was buried deep in the pocket, while the free N-terminus was located at the receptor surface, allowing N-terminal modifications. In contrast, in the C-out mode, the C-terminal carboxamide interacted with an extracellular loop, while the N-terminus was buried deep in the pocket.<sup>28</sup> In addition, all structure–activity relationship studies performed on similar hexapeptides clearly indicated that only small changes in their structure could result in different binding modes and different behaviors at the ghrelin receptor. Hence, (a) the core C-terminal pentapeptide wFWLL-NH<sub>2</sub> induced a combined agonist and inverse agonist response,<sup>20</sup> (b) addition of a single N-terminal amino acid or small modifications in the aromatic sequence -wFw- converted the core peptide into either pure agonists or pure inverse agonists,<sup>19,29</sup> and (c) ligands of the ghrelin receptor could induce a bias agonist or inverse agonist response by selectively activating or blocking one of the signaling pathways (Gaq, Gai/o, Gα12/13, and arrestin recruitment).<sup>30</sup> Last, in a recent study, a PEG or a palmitoyl group were introduced at Lys<sup>1</sup> or Lys<sup>6</sup> of the hexapeptide analogue K-(D-Bth)-FWLK-NH<sub>2</sub>.<sup>31</sup> While PEGylation decreased both binding and potency and palmitoylation led to high potency and binding affinity, the position of the modification (N- or C-terminal) did not influence the binding nor the potency at the ghrelin receptor. Hence, longer analogues such as dual peptides **4c–d** and **5a–b** and the palmitoylated analogues mentioned above may bind the ghrelin receptor in the C-in or C-out mode or in an alternative manner that would be worth investigating in the future.

However, all dual peptides showed low nanomolar potencies at the  $Y_2$  receptor. Hence, as previously reported, truncation of the large N-terminal segment [3–22] of PYY(3–36) did not affect potency at the  $Y_2$  receptor but decreased efficacy.<sup>23,26</sup> Accordingly, monomers Ac-[X<sup>23</sup>,L<sup>31</sup>]-PYY(23–36) with Lys<sup>23</sup> (**2b**) or Dpr<sup>23</sup> (**2c**) were very potent  $Y_2$  receptor agonists, although less efficient than the control hPYY(13–36). In addition, elongation at Lys<sup>23</sup> or Dpr<sup>23</sup> side chains affected potency as dual peptides **4c–d** and **5a–b** were less potent, although still in the nanomolar range, than their corresponding monomers. Except for **5a**, binding affinities of the dual peptides **4c–d** (C-ter/N-ter linked) and **5b** (N-ter/N-ter linked) followed the same trend with only a 3- to 5-fold decrease compared to the control.

Importantly, monomers selective to the  $Y_2$  receptor were inactive at the ghrelin receptor and vice versa. The potency of all dual peptides toward both receptors is thus solely induced by the moiety selective to the corresponding receptor. Moreover, as already mentioned, selectivity at the  $Y_2$ R was evaluated as Y receptors involved in the regulation of energy homeostasis induced opposite effects.  $Y_1$  and  $Y_5$  receptors promoted orexigenic signaling in the brain and periphery, whereas  $Y_4$  as  $Y_2$  promoted anorexigenic signaling. In this study, only the N-ter/N-ter linked dual peptides **5a–b** presented a net selectivity for  $Y_2$ R compared to all other Y receptors.

To summarize, the dual peptide **5a** combined the highest inverse agonist potency at the ghrelin receptor with a high agonist potency and a high selectivity at the  $Y_2$  receptor. Although lower than endogenous ligands, its binding affinity at both receptors remained in the nanomolar range. Last, **5a** is the best balanced dual peptide as it presented a shift in potencies at both receptors in the same order of magnitude than the respective controls (5 to 7-fold). Thus, **5a** was selected for further *in vivo* studies.

In order to understand the *in vivo* behavior of the dual peptide **5a**, food intake studies were performed on diet-induced obese C57BL/6 mice. Randomized groups of freely fed mice were treated with the ghrelin receptor inverse agonist **1a**, the  $Y_2$  receptor agonist **2a**, PYY(3–36), the simultaneous administration of **1a** + **2a**, or the dual peptide **5a**. In parallel, stability studies were performed on radiotracers **6–8c**, respectively, derived from **2a**, PYY(3–36), and **5a**. Except for the dual peptide **5a**, no significant differences in food intake or body weight were observed compared to those of the control group, in acute or chronic studies. Stability studies and previous food intake studies performed on monomers **1a** and **2a** need to be considered to discuss these results.

Two articles assessed the very high stability of peptides structurally close to **1a**, the hexapeptide K-(D-Bth)-FwLL-NH<sub>2</sub> and the radiotracer NODAGA(Ga)<sup>68</sup>-KwFwLL-NH<sub>2</sub>.<sup>27,31</sup> Nevertheless, **1a** did not show any effect on food intake in the present study, although it was previously reported to significantly decrease food intake for 2 h after intracerebroventricular injection in rats.<sup>19</sup> In this respect, one might hypothesize that crossing of the blood–brain barrier is required for ghrelin receptor inverse agonists to influence food intake. A recent report supported this theory with the demonstration that CNS exposure was necessary to obtain reduced food intake after oral administration of an acylurea inverse agonist in mice via a mechanism involving the ghrelin receptor.<sup>32</sup> In this context, further studies would have to assess the therapeutic potential of **1a** and understand its mode of action.

The  $Y_2$ R agonist **2a** was previously developed and showed a small reduction of food intake in lean C57BL/6 male mice in fast-refed studies over 24 h.<sup>25</sup> Moreover, a PEG-20 analogue of **2a** induced a sustained reduction of food intake and body weight in diet-induced mice for 40 days.<sup>24</sup> In the present stability studies, tracer **7c**, derived from **2a**, showed an instant degradation in blood. Interestingly, tracer **6c**, derived from PYY(3–36), stayed intact at least for 30 min after injection. It is important to mention that PYY belongs to the PP-fold peptide family, known to possess a surprisingly strong and well-ordered 3D structure.<sup>33,34</sup> Although the importance of the PP-fold motif for receptor recognition and selectivity is well established, little is known about its impact on the *in vivo* behavior of NPY derived hormones. The present stability study clearly showed that truncation of the N-terminal segment [1–23] directly affects *in vivo* stability of the peptide. In this context, the lack of biological effect of **2a** was to be expected. Importantly, PYY(3–36) did not show any effect on food intake in our study. As reproducibility of food intake experiments was reported to be hazardous for PYY(3–36) and highly discussed a few years ago, no assumption will be drawn in regard to the present results.<sup>35</sup>

Finally, only the dual peptide **5a** could induce a significant, but small in magnitude, reduction of food intake after 10 days of treatment with subcutaneous osmotic pumps slowly releasing the drugs. Interestingly, no effect was observed with a daily injection of the drug for 10 days. Moreover, no decrease in

body weight was detected either with the daily injection or with subcutaneous osmotic pumps. Tracer **8c**, derived from **5a**, showed a moderate stability in blood that could explain the discrepancies shown in the two chronic food intake studies. The slow but continuous release of the drug from the subcutaneous chambers could have offset the poor stability of the peptide that could not reach its biological effect when injected once daily.

To conclude, it is remarkable that only the dual peptide **5a** showed biological activity *in vivo*. Compounds **1a** and **2a** indeed displayed higher potencies than **5a** *in vitro*, respectively, at the ghrelin and the  $Y_2$  receptor. However, neither **1a** nor **2a** independently, nor the combination of **1a** + **2a**, induced any effect on food intake in mice. In fact, the dual peptide **5a** presented an intermediate metabolic stability between **1a** (very stable) and **2a** (unstable). Thus, the combination of the two moieties **1a** and **2a** in a single multitarget peptide **5a** balanced their respective metabolic stabilities and led to a biological response, i.e., a reduction of food intake in mice. Although further studies need to be performed to understand its mode of action and assess its activity, the dual peptide **5a** was rationally designed to selectively target ghrelin and  $Y_2$  receptors and appears as a promising lead for new antiobesity treatment.

## ■ EXPERIMENTAL PROCEDURES

**Materials.** Fmoc amino acid derivatives, diisopropylcarbodiimide (DIC), 1-hydroxybenzotriazole (HOBt), Oxyma, and Rink amid resin, were purchased from Iris Biotech (Marktredwitz, Germany) or Novabiochem (Läufelfingen, Switzerland). If not specified, the side chain protecting groups are *t*Bu for Glu, Ser, Thr, and Tyr; Boc for Lys and D-Trp; Trt for Gln; and His and Pbf for Arg. Thioanisole, *p*-thiocresol, ethandithiol, piperidine, hydrazine monohydrate, 4-dimethylaminopyridine (DMAP), triisopropylsilane (TIS), and *tert*-butanol were purchased from Fluka (Taufkirchen, Germany). Dichloromethane (DCM) and *N,N*-dimethylformamide (DMF) were purchased from Biosolve (Valkenswaard, The Netherlands). Palmitic acid, trifluoroacetic acid (TFA), acetic anhydride, diisopropylethylamine (DIPEA), octanoic acid, and Ga(NO<sub>3</sub>)<sub>3</sub> were obtained from Sigma-Aldrich (Taufkirchen, Germany). NODAGA(*t*Bu)<sub>3</sub> (4-(4,7-bis(2-*tert*-butoxy-2-oxoethyl)-1,4,7-triazonan-1-yl)-5-*tert*-butoxy-5-oxopentanoic acid) was obtained from CheMatec (Dijon, France). Gradient-grade high-performance liquid chromatography (HPLC) solvent acetonitrile (ACN) was from VWR (Darmstadt, Germany). All reagents and solvents were used without purification as provided from the commercial suppliers. For cell culture and *in vitro* assays, Dulbecco's phosphate buffered saline without calcium and magnesium (PBS), DMEM, high glucose (4.5 g·L<sup>-1</sup>) with L-glutamine, heat-inactivated fetal bovine serum (FBS), penicillin/streptavidin, and trypsin/EDTA (1:250) were purchased from PAA (Pasching, Austria). Metafectene was purchased from Biontex (Martinsried, Germany). myo-[<sup>3</sup>H] Inositol (681 MBq·mmol<sup>-1</sup>; 25.0 Ci·mmol<sup>-1</sup>) was from GE Healthcare Europe GmbH (Braunschweig, Germany). <sup>125</sup>I-ghrelin and <sup>125</sup>I-PYY are from PerkinElmer. Cell culture flasks (75 cm<sup>2</sup>) and 24-well plates were from TPP (Trasadingen, Switzerland).

**Instruments.** Automated peptide synthesis was performed with a multiple peptide synthesizer (Syro, MultiSynTech, Bochum, Germany, and ResPep SL, Intavis, Cologne, Germany for conjugates **6–8a**). Preparative HPLC was performed using a Merck-Hitachi system equipped with a C18 column (Phenomenex Jupiter 10u Proteo 90 Å: 250 × 21.2 mm, 7.8 μm, 90 Å). Analytical HPLC was performed using a Merck-Hitachi instrument equipped with a C18 column (Phenomenex Jupiter 4u Proteo 90 Å: 250 × 4.6 mm, 4 μm, 90 Å). All peptides were analyzed by matrix-assisted LASER desorption/ionization–time-of-flight (MALDI-ToF) using a Bruker Daltonics Ultraflex III mass spectrometer.

Conjugates **6–8a** were purified with preparative HPLC (ProStar, Agilent Technologies, Santa Clara, Unites States) equipped with a



preparative C18 column (Phenomenex AXIA: 250 × 30 mm, 10  $\mu$ m, 100 Å, Torrance, Unites States) and analyzed by LC-MS (LC: Agilent 1100 Series and MS: ESI Finnigan MAT) equipped with a C18 column (Phenomenex Kinetex 5  $\mu$ m C18 100 Å: 100 × 4.6 mm, 5  $\mu$ m, 100 Å).

The 1.85-GBq (50-mCi)  $^{68}\text{Ge}/^{68}\text{Ga}$  generator was purchased from iThemba Laboratories with the  $^{68}\text{Ge}$  on a  $\text{SnO}_2$ -cartridge and eluted according to the manufacturer's recommendations using a remote-controlled module.

**Peptide Synthesis.** Peptide synthesis was performed with an automated peptide synthesizer and following an Fmoc/*t*-Bu strategy as previously described.<sup>36</sup> Rink amide resin (13.5  $\mu$ mol) was used for all compounds except 1b–c, which were obtained using, respectively, preloaded Asn-Wang and Gln-Wang resins. Special amino acids were coupled manually with 5 equiv of Fmoc-amino acid, 5 equiv of DIC, and 5 equiv of HOBt or Oxyma in DMF. Completion of the coupling reactions was checked with a Kaiser test.

**Selective Dde Cleavage.** Selective Dde cleavage was performed by incubating the resin 10 times with 500  $\mu$ L of a hydrazine solution 2% in DMF (v/v) for 10 min.

**Selective Mtt Cleavage.** Selective Mtt cleavage was achieved by incubating the resin 10 times with 500  $\mu$ L of the cleavage solution, TFA/TIS/DCM: 1/5/97 (v/v/v), for 2 min.

**Introduction of a Succinic Linker.** Introduction of a succinic linker was performed to afford 1f–g, 5a–b, and 8a. Resins of the corresponding precursors were incubated with 10 equiv of succinic anhydride and 10 equiv of  $\text{NEt}_3$  overnight in DMF.

**N-Terminal Acylation.** N-Terminal acylation was performed to afford 2b–c, 4a–c, 5a–b, and 7–8a. Resins of the corresponding precursors were incubated with 10 equiv of acetic anhydride and 10 equiv of  $\text{NEt}_3$  for 30 min in DMF.

**Introduction of the Bifunctional Chelator NODAGA.** Introduction of the bifunctional chelator NODAGA was performed to afford 6–8a. The corresponding precursors were incubated with 2 equiv of NODAGA(*t*Bu)<sub>3</sub> and 2 equiv of HOBt overnight in DMF.

**Cleavage from the Resin and Simultaneous Side Chain Deprotections.** Cleavage from the resin and simultaneous side chain deprotections were performed by incubating the resins for 3 h with 900  $\mu$ L of TFA and 100  $\mu$ L of a scavenger mixture: thioanisole/1,2-ethanedithiol, 7/3 (v/v), for peptides containing a tryptophan residue and thiocresol for all other peptides. Peptides were precipitated in ice-cold diethyl ether or a mixture of hexane/diethyl ether 3/1 (v/v) and lyophilized.

**Purification.** Purification of peptides was performed by preparative RP-HPLC using a C18 column (Phenomenex Jupiter 10u Proteo 90 Å: 250 mm × 21.2 mm, 7.8  $\mu$ m, 90 Å). Conjugates 6a–c were purified using a preparative C18 column (Phenomenex AXIA: 250 × 30 mm, 10  $\mu$ m, 100 Å). Different linear gradient systems were used with water + 0.1% TFA and ACN + 0.08% TFA at a flow rate of 10 mL·min<sup>−1</sup>. The identity of peptides 1b–g, 2b–c, 4a–d, and 5a–b was confirmed by MALDI-ToF mass spectrometry and by LC-MS with electrospray ionization for 6–8a. The purity of all compounds was determined by analytical RP-HPLC and was higher than 95%.

**Complexation with Ga for the *in Vitro* Assay.** Complexation with Ga for the *in vitro* assay was performed to afford the NODAGA(Ga)-chelates 6–8b. Then, 0.5  $\mu$ mol of the NODAGA-peptide conjugates 6–8a was dissolved in 700  $\mu$ L of an ammonium acetate solution (0.1 M in H<sub>2</sub>O). Three hundred microliters of a Ga(NO<sub>3</sub>)<sub>3</sub> solution (0.04 M in H<sub>2</sub>O) was added, and the pH adjusted to 4.5 with diluted HCl. The solutions were then incubated for 30 min at 37 °C and directly purified by preparative HPLC to obtain 6–8b.

**TFA-HCl Exchange for *in Vivo* Assays.** The peptides (15  $\mu$ mol) were incubated three times in a 50 mM HCl solution in H<sub>2</sub>O (4 mL) at room temperature for 1 h and then lyophilized. Integrity and purity of the compounds were controlled by MALDI-ToF MS and HPLC.

**$^{68}\text{Ga}$ -Production and Radiolabeling.**  $^{68}\text{Ga}$ -Production and radiolabeling of 6–8a to afford radiotracers 6–8c were performed according to procedures previously described in detail.<sup>27</sup> Briefly,  $^{68}\text{Ga}$  ( $T_{1/2}$  = 68 min,  $\beta^+$  = 89%, and EC = 11%) was available from  $^{68}\text{Ge}/^{68}\text{Ga}$ -generator-systems to afford a solution of  $^{68}\text{Ga}(\text{OAc})_3$  of pH

4.0–4.5. The solution was added to 20 nmol of 6–8a in acetate buffer for 15 min at 37 °C to afford [ $^{68}\text{Ga}$ ]-labeled 6–8c in solution with radiochemical purity higher than 95%. Before formulation for the *in vitro* or *in vivo* application solutions were filtrated and diluted with electrolyte solution E-153 (140 mMol Na<sup>+</sup>, 5 mMol K<sup>+</sup>, 2.5 mMol Ca<sup>2+</sup>, 1.5 mMol Mg<sup>2+</sup>, 50 mMol acetate, and 103 mMol Cl<sup>−</sup>) to reach a concentration of about 80 MBq·mL<sup>−1</sup> and directly used for the stability studies.

**Inositol Triphosphate Turnover Assay.** The inositol triphosphate turnover assay was performed on COS-7 cells stably expressing the human ghrelin receptor (GHS-R1a) or coexpressing the human Y<sub>2</sub> receptor and a chimeric G<sub>i/q</sub> protein.<sup>36,37</sup> All signal transduction assays were performed in duplicate and repeated at least two times independently. For experiments, COS-7 cells were seeded out in 24-well plates (80.000–100.000 cells per well) in DMEM with 10% FCS and incubated with 4  $\mu$ Ci·mL<sup>−1</sup> of myo-[<sup>3</sup>H]-inositol (25.0 Ci·mmol<sup>−1</sup>) 1 day after seeding. After 16 h, cells were stimulated for 2 h with six or seven different concentrations of the peptides in DMEM containing 10 mM LiCl and 0.1% BSA. The stimulation was stopped by aspiration of the medium. After cell lysis and removal of cell debris, intracellular inositol phosphate levels were determined by anion-exchange chromatography. For each experiment, at least three wells were left nonstimulated and expressed the basal activity of the receptor. For COS-7 cells stably expressing the human ghrelin receptor, the nonstimulated cells reflected the constitutive activity of the receptor. EC<sub>50</sub>, pEC<sub>50</sub>, and E<sub>max</sub> values were obtained from log(concentration)–response curves according to a 4 parameter logistic (4PL) nonlinear regression model using GraphPad Prism 6.0 program (GraphPad Software, San Diego, USA). Accordingly, for the ghrelin receptor, the raw DPM values (disintegrations per minute) were normalized as % of constitutive activity of the ghrelin receptor, the top best-fit values from log(concentration)–response curves of each compound being defined as 100% of constitutive activity of the ghrelin receptor. For the Y<sub>2</sub> receptor, raw DPM values were normalized as % of maximum activity of the Y<sub>2</sub> receptor, the bottom and top best-fit values from the log(concentration)–response curve of PYY(13–36) being defined as 0% and 100% of the maximum activity of the Y<sub>2</sub> receptor. Raw and normalized data were analyzed

**Selectivity of Dual Peptides 4c–d and 5a–b at Y<sub>2</sub> Receptors.**

Selectivity of dual peptides 4c–d and 5a–b at Y<sub>2</sub> receptors was also performed by measurement of inositol triphosphate accumulation in COS-7 cells stably expressing the respective hY receptor subtype and a chimeric G<sub>i/q</sub> protein. The cells were stimulated with 10<sup>−6</sup> M of each peptide after incubation with 4  $\mu$ Ci·mL<sup>−1</sup> of myo-[<sup>3</sup>H]-inositol (25.0 Ci·mmol<sup>−1</sup>) as described above. Each cell line was also stimulated with eight different concentrations of NPY to obtain a control concentration–response curve for each receptor. All experiments were performed in duplicate and repeated at least two times independently.

**Competitive Receptor Binding Assays.** Competitive receptor binding assays were carried using stably transfected COS7 cells expressing the eYFP-fused human ghrelin receptor (10.000/vial) or HEK293 cells stably transfected with the human Y<sub>2</sub>-receptor-eYFP fusion protein (40.000/vial). Cells were detached with trypsin/EDTA and resuspended in DMEM containing 1% BSA and 50  $\mu$ M Pefabloc. Peptides were dissolved in 1% BSA/H<sub>2</sub>O. Binding was carried out in the presence of 60 pM [<sup>125</sup>I]-ghrelin or 80 pM [<sup>125</sup>I]-PYY, respectively. Competition of binding sites was achieved by incubating with increasing concentrations of peptides (10<sup>−5</sup> to 10<sup>−11</sup> M) for 75 min at room temperature (ghrelin receptor) or for 2 h on ice (Y<sub>2</sub> receptor). Cells were washed with ice-cold PBS. IC<sub>50</sub> values of the binding curves were determined in triplicate, calculated with GraphPad Prism 5.0, and given as the mean ± SEM of at least two independent experiments.

**Animal Experiments.** The investigation conforms to the Guide for the Care and Use of Laboratory Animals published by the US National Institutes of Health (NIH Publication No. 85–23, revised 1996) and was approved by the local authorities of the state of Saxony (Regierungspräsidium Leipzig and Dresden), Germany as recommended by the responsible local animal ethics review board (TVV05/13; 24-9168.21-4/2004-1).

**Food Intake Assays.** Thirty female C57BL/6J mice were purchased from Janvier (Genest Saint Isle, France). All mice were kept acclimatized at 22 °C + 2 °C and with a 12-h light-dark cycle, as well as free access to food (standard chow) and water.

**Chronic IP Application.** After an adaptation period of 3 weeks, mice were randomly divided into six groups. Each group received an IP daily injection of a saline solution (control group), **1a**, PYY(3–36), **2a**, **1a** + **2a**, or **5a** at 100 nM/kg over a period of 10 days. Body weight and food intake of each mouse were monitored daily.

**Chronic Subcutaneously Infusion.** After an adaptation period of 3 weeks mice were randomly divided into 6 groups and were implanted with Alzet osmotic micropumps (Durect Corporation, Cupertino, USA). Osmotic pumps were filled with a saline solution (control group), **1a**, PYY(3–36), **2a**, **1a** + **2a**, or **5a** delivering 6 nmol of drug per day. The pumps were implanted dorsally under the skin under light ether anesthesia. The body weight and food intake of each mouse were monitored daily during the 14 days of treatment.

**Statistical Analysis.** Repeated-measures two way analysis of variance (rANOVA) analyses were performed to assess the significance of the effects of drug treatments, time, and interaction between drug treatment and time for the cumulative food intake and body weight. Drug treatment was considered as in-between subject factor and time as within subject factor. When rANOVA tests were significant, posthoc Dunnett's multiple comparison at each time-point was performed, and the resulting *p*-values were adjusted for multiple hypotheses testing. Analyses were carried out with the GraphPad Prism 6.0 program (GraphPad Software, San Diego, USA).

**In Vivo Stability Assays.** *In Vivo* stability assays were performed for radiotracers **6–8c** on male Wistar rats according to a procedure previously described.<sup>27</sup> Arterial blood samples were collected at different times after injections, and the activity (% ID·mL<sup>-1</sup>) was measured to give the arterial blood activity of **6–8c**. Blood cells were separated by centrifugation (5 °C, 5 min, 8000 rpm), and plasma proteins were precipitated using 60% acetonitrile and subsequent centrifugation (5 °C, 5 min, 8000 rpm). The supernatant was analyzed by radio-HPLC. The radio-HPLC system (Agilent 1100 series) applied for metabolite analysis was equipped with UV detection (254 nm) and an external radiochemical detector (Ramona, Raytest GmbH, Straubenhardt, Germany). Analysis was performed on a Zorbax C18 300SB (250 × 9.4 mm; 4 μm) column with an eluent system C (water +0.1% TFA) and D (acetonitrile +0.1% TFA) in a gradient 5 min 95% C, 10 min to 95% D, and 5 min at 95% D at a flow rate of 3 mL·min<sup>-1</sup>. HPLC was performed on **6–8c** added to a rat blood sample and arterial blood samples from 1 to 120 min after injections. The metabolite fraction in blood was calculated as a fraction of the parent compound in plasma in HPLC.

## ■ ASSOCIATED CONTENT

### ■ Supporting Information

Analytical data with RP-HPLC retention times and molecular masses of the synthesized peptides; and tabular results and figures of chronic food intake assays not shown in the manuscript. The Supporting Information is available free of charge on the ACS Publications website at DOI: 10.1021/jm501702q.

## ■ AUTHOR INFORMATION

### Corresponding Author

\*Phone: +49 221 470 3175. E-mail: cchollet@uni-koeln.de.

### Present Address

\*(C.C.) Institute of Biochemistry, University of Cologne, Zùlpicher Strasse 47, 50674 Cologne, Germany.

### Notes

The authors declare no competing financial interest.

## ■ ACKNOWLEDGMENTS

We thank Regina Reppich-Sacher and Kristin Loebner for technical assistance during the synthesis and *in vitro* experiments, Regina Herrlich, Andrea Suhr, and Eva Böge for technical assistance in the animal experiments, peptide radiolabeling, and metabolite analysis, Dr. Marit Ackermann for discussions on statistical analysis, and Professor Ines Neundorff for scientific discussions and support. This project was financially supported by the EU (Gastrointestinal Peptides in Obesity, GIPIO, Grant Agreement Number 223057), the BMBF (IFB Adipositas Diseases K7-18, Adi KOSb to N.K.), by a grant from Deutsche Forschungsgemeinschaft SFB1052/1, "ObesityMechanisms," and the Alexander von Humboldt foundation. Y.Z. is grateful for the funding through the BMBF grant 03Z2EN12 and BMBF BioLithoMorphie project 03Z2E511.

## ■ ABBREVIATIONS USED

AgRP, agouti-related peptide; Boc, *tert*-butoxycarbonyl; D-Bth,  $\beta$ -(3-benzothienyl)-D-alanine; DIC, *N,N'*-diisopropylcarbodiimide; D-1-Nal, D-1-naphthylalanine; DMF, dimethylformamide; FCS, fetal calf serum; Fmoc, 9-fluorenylmethoxycarbonyl; GHS-R, growth hormone secretagogue receptor; HOBt, 1-hydroxybenzotriazole; Mtt, 4-methyltrityl; NODAGA, 1,4,7-triazacyclononane,1-glutaric acid-4,7-acetic acid; NODAGA-(tBu)<sub>3</sub>, 4-(4,7-bis(2-(*tert*-butoxy)-2-oxoethyl)-1,4,7-triazacyclononan-1-yl)-5-(*tert*-butoxy)-5-oxopentanoic acid; NPY, neuropeptide Y; SAR, structure–activity relationship; *t*Bu, *tert*-butyl; TFA, trifluoroacetic acid; Trt, trityl

## ■ REFERENCES

- (1) Field, B. C. T.; Chaudhri, O. B.; Bloom, S. R. Bowels Control Brain: Gut Hormones and Obesity. *Nat. Rev. Endocrinol.* **2010**, *6*, 444–453.
- (2) Morton, G. J.; Cummings, D. E.; Baskin, D. G.; Barsh, G. S.; Schwartz, M. W. Central Nervous System Control of Food Intake and Body Weight. *Nature* **2006**, *443*, 289–295.
- (3) Valentino, M. A.; Lin, J. E.; Waldman, S. A. Central and Peripheral Molecular Targets for Antiobesity Pharmacotherapy. *Clin. Pharmacol. Ther.* **2010**, *87*, 652–662.
- (4) Troke, R. C.; Tan, T. M.; Bloom, S. R. The Future Role of Gut Hormones in the Treatment of Obesity. *Ther. Adv. Chronic Dis.* **2014**, *5*, 4–14.
- (5) Chaudhri, O. B.; Wynne, K.; Bloom, S. R. Can Gut Hormones Control Appetite and Prevent Obesity? *Diabetes Care* **2008**, *31*, S284–S289.
- (6) Delzenne, N.; Blundell, J.; Brouns, F.; Cunningham, K.; De Graaf, K.; Erkner, A.; Lluch, A.; Mars, M.; Peters, H. P. F.; Westerterp-Plantenga, M. Gastrointestinal Targets of Appetite Regulation in Humans. *Obes. Rev.* **2010**, *11*, 234–250.
- (7) Diniz, M. F. H. S.; Azeredo Passos, V. M.; Diniz, M. T. C. Bariatric Surgery and the Gut-Brain Communication—The State of the Art Three Years Later. *Nutrition* **2010**, *26*, 925–931.
- (8) Berthoud, H.-R.; Shin, A. C.; Zheng, H. Obesity Surgery and Gut–brain Communication. *Physiol. Behav.* **2011**, *105*, 106–119.
- (9) Murphy, K. G.; Dhillo, W. S.; Bloom, S. R. Gut Peptides in the Regulation of Food Intake and Energy Homeostasis. *Endocr. Rev.* **2006**, *27*, 719–727.
- (10) Schwartz, M. W.; Morton, G. J. Obesity: Keeping Hunger at Bay. *Nature* **2002**, *418*, 595–597.
- (11) Bloom, S. R.; Kuhajda, F. P.; Laher, I.; Pi-Sunyer, X.; Ronnett, G. V.; Tan, T. M. M.; Weigle, D. S. The Obesity Epidemic: Pharmacological Challenges. *Mol. Interv.* **2008**, *8*, 82–98.
- (12) Zinman, B. Initial Combination Therapy for Type 2 Diabetes Mellitus: Is It Ready for Prime Time? *Am. J. Med.* **2011**, *124*, S19–S34.



- (13) Field, B. C. T.; Wren, A. M.; Peters, V.; Baynes, K. C. R.; Martin, N. M.; Patterson, M.; Alsarraf, S.; Amber, V.; Wynne, K.; Ghatei, M. A.; Bloom, S. R. PYY3–36 and Oxyntomodulin Can Be Additive in Their Effect on Food Intake in Overweight and Obese Humans. *Diabetes* **2010**, *59*, 1635–1639.
- (14) Anighoro, A.; Bajorath, J.; Rastelli, G. Polypharmacology: Challenges and Opportunities in Drug Discovery. *J. Med. Chem.* **2014**, *57*, 7874–7887.
- (15) Leite-Moreira, A. F.; Soares, J.-B. Physiological, Pathological and Potential Therapeutic Roles of Ghrelin. *Drug Discovery Today* **2007**, *12*, 276–288.
- (16) Tharakan, G.; Tan, T.; Bloom, S. Emerging Therapies in the Treatment of “Diabetes”: Beyond GLP-1. *Trends Pharmacol. Sci.* **2011**, *32*, 8–15.
- (17) Karra, E.; Chandarana, K.; Batterham, R. L. The Role of Peptide YY in Appetite Regulation and Obesity. *J. Physiol.* **2009**, *587*, 19–25.
- (18) Chollet, C.; Meyer, K.; Beck-Sickinger, A. G. Ghrelin—A Novel Generation of Anti-obesity Drug: Design, Pharmacomodulation and Biological Activity of Ghrelin Analogues. *J. Pept. Sci.* **2009**, *15*, 711–730.
- (19) Els, S.; Schild, E.; Petersen, P. S.; Kilian, T.-M.; Mokrosinski, J.; Frimurer, T. M.; Chollet, C.; Schwartz, T. W.; Holst, B.; Beck-Sickinger, A. G. An Aromatic Region To Induce a Switch between Agonism and Inverse Agonism at the Ghrelin Receptor. *J. Med. Chem.* **2012**, *55*, 7437–7449.
- (20) Holst, B.; Lang, M.; Brandt, E.; Bach, A.; Howard, A.; Frimurer, T. M.; Beck-Sickinger, A.; Schwartz, T. W. Ghrelin Receptor Inverse Agonists: Identification of an Active Peptide Core and Its Interaction Epitopes on the Receptor. *Mol. Pharmacol.* **2006**, *70*, 936–946.
- (21) Servin, A. L.; Rouyer-Fessard, C.; Balasubramaniam, A.; Pierre, S. S.; Laburthe, M. Peptide-YY and Neuropeptide-Y Inhibit Vasoactive Intestinal Peptide-Stimulated Adenosine 3',5'-Monophosphate Production in Rat Small Intestine: Structural Requirements of Peptides for Interacting with Peptide-YY-Preferring Receptors. *Endocrinology* **1989**, *124*, 692–700.
- (22) Pedragosa Badia, X.; Stichel, J.; Beck-Sickinger, A. G. Neuropeptide Y Receptors: How to Get Subtype Selectivity. *Neuroendocr. Sci.* **2013**, *4*, 5.
- (23) Potter, E. K.; Barden, J. A.; McCloskey, M. J. D.; Selbie, L. A.; Tseng, A.; Herzog, H.; Shine, J. A Novel Neuropeptide Y Analog, N-Acetyl [Leu28, Leu31]neuropeptide Y-(24–36), with Functional Specificity for the Presynaptic (Y2) Receptor. *Eur. J. Pharmacol. Mol. Pharmacol.* **1994**, *267*, 253–262.
- (24) Ortiz, A. A.; Milardo, L. F.; DeCarr, L. B.; Buckholz, T. M.; Mays, M. R.; Claus, T. H.; Livingston, J. N.; Mahle, C. D.; Lumb, K. J. A Novel Long-Acting Selective Neuropeptide Y2 Receptor Polyethylene Glycol-Conjugated Peptide Agonist Reduces Food Intake and Body Weight and Improves Glucose Metabolism in Rodents. *J. Pharmacol. Exp. Ther.* **2007**, *323*, 692–700.
- (25) DeCarr, L. B.; Buckholz, T. M.; Milardo, L. F.; Mays, M. R.; Ortiz, A.; Lumb, K. J. A Long-Acting Selective Neuropeptide Y2 Receptor PEGylated Peptide Agonist Reduces Food Intake in Mice. *Bioorg. Med. Chem. Lett.* **2007**, *17*, 1916–1919.
- (26) Cabrele, C.; Beck-Sickinger, A. G. Molecular Characterization of the Ligand–Receptor Interaction of the Neuropeptide Y Family. *J. Pept. Sci.* **2000**, *6*, 97–122.
- (27) Chollet, C.; Bergmann, R.; Pietzsch, J.; Beck-Sickinger, A. G. Design, Evaluation, and Comparison of Ghrelin Receptor Agonists and Inverse Agonists as Suitable Radiotracers for PET Imaging. *Bioconjugate Chem.* **2012**, *23*, 771–784.
- (28) Sivertsen, B.; Lang, M.; Frimurer, T. M.; Holliday, N. D.; Bach, A.; Els, S.; Engelstoft, M. S.; Petersen, P. S.; Madsen, A. N.; Schwartz, T. W.; Beck-Sickinger, A. G.; Holst, B. Unique Interaction Pattern for a Functionally Biased Ghrelin Receptor Agonist. *J. Biol. Chem.* **2011**, *286*, 20845–20860.
- (29) Holst, B.; Mokrosinski, J.; Lang, M.; Brandt, E.; Nygaard, R.; Frimurer, T. M.; Beck-Sickinger, A. G.; Schwartz, T. W. Identification of an Efficacy Switch Region in the Ghrelin Receptor Responsible for Interchange between Agonism and Inverse Agonism. *J. Biol. Chem.* **2007**, *282*, 15799–15811.
- (30) Sivertsen, B.; Holliday, N.; Madsen, A. N.; Holst, B. Functionally Biased Signalling Properties of 7TM Receptors – Opportunities for Drug Development for the Ghrelin Receptor. *Br. J. Pharmacol.* **2013**, *170*, 1349–1362.
- (31) Kostelnik, K. B.; Els-Heindl, S.; Klötting, N.; Baumann, S.; von Bergen, M.; Beck-Sickinger, A. G. High Metabolic in Vivo Stability and Bioavailability of a Palmitoylated Ghrelin Receptor Ligand Assessed by Mass Spectrometry. *Bioorg. Med. Chem.* **2014**, DOI: 10.1016/j.bmc.2014.12.008.
- (32) McCoull, W.; Barton, P.; Brown, A. J. H.; Bowker, S. S.; Cameron, J.; Clarke, D. S.; Davies, R. D. M.; Dossetter, A. G.; Ertan, A.; Fenwick, M.; Green, C.; Holmes, J. L.; Martin, N.; Masters, D.; Moore, J. E.; Newcombe, N. J.; Newton, C.; Pointon, H.; Robb, G. R.; Sheldon, C.; Stokes, S.; Morgan, D. Identification, Optimization, and Pharmacology of Acylurea GHS-R1a Inverse Agonists. *J. Med. Chem.* **2014**, *57*, 6128–6140.
- (33) Bjoernholm, B.; Joergensen, F. S.; Schwartz, T. W. Conservation of a Helix-Stabilizing Dipole Moment in the PP-Fold Family of Regulatory Peptides. *Biochemistry (Moscow)* **1993**, *32*, 2954–2959.
- (34) Nygaard, R.; Nielbo, S.; Schwartz, T. W.; Poulsen, F. M. The PP-Fold Solution Structure of Human Polypeptide YY and Human PYY3–36 As Determined by NMR. *Biochemistry (Moscow)* **2006**, *45*, 8350–8357.
- (35) Boggiano, M. M.; Chandler, P. C.; Oswald, K. D.; Rodgers, R. J.; Blundell, J. E.; Ishii, Y.; Beattie, A. H.; Holch, P.; Allison, D. B.; Schindler, M.; Arndt, K.; Rudolf, K.; Mark, M.; Schoelch, C.; Joost, H. G.; Klaus, S.; Thöne-Reineke, C.; Benoit, S. C.; Seeley, R. J.; Beck-Sickinger, A. G.; Koglin, N.; Raun, K.; Madsen, K.; Wulff, B. S.; Stidsen, C. E.; Birringer, M.; Kreuzer, O. J.; Deng, X. Y.; Whitcomb, D. C.; Halem, H.; Taylor, J.; Dong, J.; Datta, R.; Culler, M.; Ortmann, S.; Castañeda, T. R.; Tschöp, M. PYY3–36 as an Anti-obesity Drug Target. *Obes. Rev.* **2005**, *6*, 307–322.
- (36) Els, S.; Beck-Sickinger, A. G.; Chollet, C. Ghrelin Receptor: High Constitutive Activity and Methods for Developing Inverse Agonists. *Methods Enzymol.* **2010**, *485*, 103–121.
- (37) Mäde, V.; Bellmann-Sickert, K.; Kaiser, A.; Meiler, J.; Beck-Sickinger, A. G. Position and Length of Fatty Acids Strongly Affect Receptor Selectivity Pattern of Human Pancreatic Polypeptide Analogues. *ChemMedChem* **2014**, *9*, 2463–2474.